Journal of Power Sources 681 (2026) 240242

Contents lists available at ScienceDirect

Journal of Power Sources

journal homepage: www.elsevier.com/locate/jpowsour

DMC-rich, low-EC, moderately concentrated electrolytes for lithium-ion batteries: Roles of solvent composition and salt concentration

Yuji Ide [a], Yanko Marinov Todorov [b], Masaki Deguchi [c], Koji Abe [a,b,*]

[a] Graduate School of Sciences and Technology for Innovation, Yamaguchi University, 2-16-1 Tokiwadai, Ube, Yamaguchi, 755-8611, Japan
[b] Organization for Research Initiatives, Yamaguchi University, 2-16-1 Tokiwadai, Ube, Yamaguchi, 755-8611, Japan
[c] Energy Research and Development Center, Panasonic Energy Co., Ltd., 1-1 Matsushita-cho, Moriguchi, Osaka, 570-8511, Japan

HIGHLIGHTS

- Separator wettability correlates with initial Coulombic efficiency in LIB cells.
- A 1.8 M LiFSI DMC-rich electrolyte exhibits good rate performance at 0 °C.
- Reduced EC content improves wettability and decreases viscosity.
- Reduced cyclic solvent content is associated with lower Al corrosion in LiFSI.
- Balanced transport and corrosion behavior are observed at 1.8 M LiFSI.

ARTICLE INFO

Keywords:
DMC-Rich electrolyte
Moderately concentrated electrolyte
Separator wettability
Aluminum current collector corrosion
Lithium-ion batteries

ABSTRACT

Ethylene carbonate (EC) plays a central role in conventional lithium-ion battery electrolytes by enabling stable SEI formation on graphite anodes. However, reducing EC content is increasingly required to improve low-temperature performance and mitigate associated drawbacks. Here, we present a systematic design strategy for low-EC electrolytes by tuning lithium salt concentration and solvent composition. A DMC-rich electrolyte composed of 1.8 M lithium bis(fluorosulfonyl)imide (LiFSI) in DMC/ethyl methyl carbonate (EMC)/EC (85/10/5, vol%) achieves a balanced combination of viscosity and ionic conductivity while maintaining sufficient wettability on polyolefin separators. Limiting the fraction of high-dielectric cyclic solvents is associated with reduced aluminum dissolution in LiFSI-based systems, as suggested by linear sweep voltammetry and inductively coupled plasma analysis. As a result, $LiNi_{0.5}Co_{0.2}Mn_{0.3}O_2$/graphite full cells operated at 4.2 V and 60 °C exhibit improved cycling stability, retaining 84% of the initial capacity after 300 cycles compared with 56% for a $LiPF_6$-based electrolyte. This study identifies a practical compositional window and provides a design-oriented framework for DMC-rich, low-EC, moderately concentrated electrolytes in lithium-ion batteries.

1. Introduction

Ethylene carbonate (EC)-based electrolytes have long been the cornerstone of lithium-ion batteries (LIBs) employing graphite anodes, as EC enables the formation of a stable solid electrolyte interphase (SEI) via reductive decomposition [1,2]. Conventionally, 1 M lithium hexafluorophosphate ($LiPF_6$) dissolved in EC/linear carbonate mixtures has been widely used, providing high ionic conductivity while suppressing aluminum (Al) current collector corrosion through the formation of protective AlF_3- and LiF-rich surface layers [3,4].

Despite these advantages, EC imposes intrinsic limitations. Its high melting point (37 °C) leads to poor low-temperature performance, and EC-rich electrolytes exhibit sluggish transport properties under sub-ambient conditions. Linear carbonates such as dimethyl carbonate (DMC), ethyl methyl carbonate (EMC), and diethyl carbonate (DEC) are therefore incorporated to reduce viscosity and improve wettability toward polyolefin separators. However, these solvents introduce trade-offs, including lower flash points and altered interfacial reactivity, complicating the simultaneous optimization of safety, transport properties, and electrochemical stability [5]. In addition, polyolefin separators (typically polypropylene (PP)/polyethylene (PE)/PP trilayers) exhibit limited affinity toward highly polar solvents, making wettability

* Corresponding author. Graduate School of Sciences and Technology for Innovation, Yamaguchi University, 2-16-1 Tokiwadai, Ube, Yamaguchi, 755-8611, Japan.
E-mail address: abekoji@yamaguchi-u.ac.jp (K. Abe).

https://doi.org/10.1016/j.jpowsour.2026.240242
Received 4 February 2026; Received in revised form 17 April 2026; Accepted 25 April 2026

a critical parameter for practical cell performance.

Previous approaches to improving separator wettability have mainly relied on electrolyte additives or separator surface modification, such as alumina coatings [6–8]. In contrast, this study focuses on controlling the primary solvent composition to simultaneously tune wettability and interfacial stability without introducing additional components.

In recent years, EC-free or DMC-based electrolyte systems have attracted increasing attention. For example, Dahn and co-workers reported that, in $LiPF_6$-based systems, EC oxidation above ~4.4 V accelerates gas evolution and impedance growth, highlighting its detrimental role under high-voltage conditions [9–16]. In contrast to $LiPF_6$-based systems, lithium bis(fluorosulfonyl)imide (LiFSI) electrolytes at conventional or moderately concentrated levels (~1–2 M) can induce severe Al current collector corrosion unless protective strategies are employed [17].

In $LiPF_6$-based systems, highly concentrated and superconcentrated electrolytes have been explored to mitigate these issues, as they expand the electrochemical stability window and suppress metal dissolution [18,19]. However, their high viscosity and cost limit practical implementation [20]. Moderately concentrated electrolytes (~2–3 M) offer a promising compromise, balancing improved interfacial stability with acceptable transport properties [21]. Nevertheless, prior studies have often investigated EC reduction and moderate salt concentration independently, leaving a gap in understanding how their combined effect governs practical properties such as separator wettability, ionic conductivity, low-temperature behavior, and Al corrosion.

Here, we systematically investigate DMC-rich, low-EC electrolytes across a range of salt concentrations. By integrating physicochemical and electrochemical evaluations, we identify a practical compositional window that simultaneously achieves balanced transport properties, sufficient wettability, and reduced aluminum dissolution without relying on superconcentrated formulations. To our knowledge, few studies have systematically integrated EC reduction with moderately concentrated salt levels and quantify its effects on both electrochemical and physicochemical properties, providing a design-oriented framework for next-generation LIB electrolytes.

This study focuses on a design-oriented approach, providing practical guidelines rather than detailed mechanistic insights.

2. Experimental

2.1. Chemical materials

$LiPF_6$ was supplied by Kanto Denka Kogyo Co., Ltd. EC, DMC, EMC, γ-butyrolactone (GBL), and LiFSI were obtained from MU Ionic Solutions Corporation. All solvent compositions are expressed on a volume (vol%) basis.

The following electrolytes were investigated: 1 M $LiPF_6$ in EC/DMC = 3/7; 1 M LiFSI in EC/DMC = 3/7; 1 M $LiPF_6$ in EC/EMC/DMC = 3/3/4; 1 M LiFSI in EC/GBL = 3/7; various LiFSI concentrations in EC/DMC = 1/2; and various LiFSI concentrations in EC/EMC/DMC = 5/10/85. All solvents were battery grade (H_2O < 10 ppm, HF < 30 ppm).

2.2. Separator wettability test

Because the separator is a porous polyolefin membrane, static contact angle measurements were unsuitable due to time-dependent liquid penetration and solvent evaporation. Therefore, wettability was evaluated by directly observing electrolyte infiltration.

A 20 μL droplet was placed on a 20-μm-thick PP/PE/PP dry trilayer separator (Ube Maxell Co., Ltd.), and the color change from white to gray was recorded after 15 s. The separator consists of relatively wettable PP outer layers and a more hydrophobic PE inner layer. As PP wets more readily than PE, incomplete penetration ("not enough" wetting) can be identified when only the PP layer is wetted.

By utilizing this intrinsic wettability difference and controlling droplet volume, the evaluation was performed under consistent conditions, enabling reproducible and reliable relative comparison among different electrolytes.

All measurements were conducted under identical experimental conditions (droplet volume, observation time, and ambient environment) to minimize variability.

Although this method is qualitative, it reflects electrolyte infiltration into porous separators, which is generally considered more relevant to practical cell performance than static contact angle measurements for porous media [6].

Importantly, the same evaluation method was consistently applied to all samples, ensuring comparability across electrolyte compositions.

2.3. Physicochemical property evaluation of solvents and electrolytes

As reported previously [6], viscosity was measured at 25 °C using a DV-I Prime LV rotational viscometer (AMETEK Brookfield) with 0.5 mL of electrolyte. Values represent the average of four measurements. Ionic conductivity was measured at 25 °C using a CM-42X conductivity meter (DKK-TOA Corporation) with 3 mL of electrolyte. The flash point was determined using a TAG4 flash point tester (Anton Paar) with 12 mL of electrolyte. For solidification testing, 3 mL of electrolyte was cooled to −20 °C, and photographs were taken 3 h after reaching the target temperature. The electrolyte density was measured at 25 °C using a DMA 4500 M densimeter (Anton Paar).

2.4. 2032-Coin cell evaluation

Coin cell charge–discharge tests were performed as described previously [22]. At least two cells were tested for each condition, and representative data are shown. In this paper, the positive and negative electrodes are referred to as the cathode and anode, respectively.

The cathode ($LiNi_{0.5}Co_{0.2}Mn_{0.3}O_2$, NCM523) was prepared by coating a slurry onto Al foil. The composition was NCM523:acetylene black (AB):polyvinylidene fluoride (PVdF) = 92:5:3 by weight. The areal loading was 9.5 mg cm^{-2}, and the electrode was calendered to a density of 2.5 g cm^{-3}.

The anode (natural graphite, NG) was coated onto copper (Cu) foil using a slurry prepared in deionized water at a weight ratio of NG: styrene–butadiene rubber (SBR):carboxymethyl cellulose (CMC) = 98:1:1. The areal density was 5.5 mg cm^{-2}, and the electrode was pressed to a density of 1.45 g cm^{-3}.

CR2032 cells (initial capacity: 2.3 mAh) were assembled using a Ø14 mm cathode, Ø15 mm anode, and a Ø19 mm, 20 μm-thick PP/PE/PP separator (Ube Maxell). A Ø16 mm glass fiber sheet (Whatman GF/A, Cytiva) was placed between the separator and cathode. The N/P ratio was ~1.3, and ~0.2 mL of electrolyte was injected.

Because the SUS316L coin cell case corrodes more readily than Al [23], a Ø19 mm, 25 μm-thick Al foil was inserted between the cathode and the case.

Cycling was conducted at 25 °C using an ACD-M01A system (ASKA Electronics Co., Ltd) at 1C-rate (1C = 2.3 mA) between 4.2 V (CC–CV) and 3.0 V (CC). In the rate test, the charge and discharge rates were identical. During the CV mode, charging was continued until the current decreased to one-tenth of the CC mode.

2.5. Linear sweep voltammetry

Al corrosion was evaluated by linear sweep voltammetry (LSV). An Al/Li/Li glass cell was assembled in an argon-filled glove box. The Al working electrode (5 mm width, 0.5 mm thickness) was immersed to a length of 16 mm in 6.5 mL of electrolyte. A potentiostat (SP-150, Biologic Science Instruments) was used to sweep the potential to 5.0 V at a scan rate of 0.5 mV s^{-1}.

2.6. Analysis of deposited Al on graphite

After 200 cycles, the coin cell was disassembled in an argon-filled glove box. The graphite electrode was rinsed twice with DMC. Half of the resulting electrode was placed in 5 mL of concentrated hydrochloric acid. After 1.5 h, the electrode was filtered using a 0.2 μm disposable membrane filter (DISMIC 25CS020AN, ADVANTEC). It was then rinsed and diluted with deionized water to a volume of 25 mL. The sample was analyzed using an inductively coupled plasma (ICP) optical emission spectrometer (ICP-OES, SPS3500, Hitachi High-Tech Co.).

3. Results and discussion

We investigated the influence of two key parameters on battery performance and electrolyte properties: (i) the EC/DMC volume ratio and (ii) the lithium salt concentration.

3.1. 1 M $LiPF_6$ EC/DMC electrolyte system

Separator wettability and electrochemical performance were first evaluated using conventional 1 M $LiPF_6$ EC/DMC electrolytes with varying EC fractions.

At an EC/DMC ratio of 6/4 (vol%), no reversible charge/discharge behavior was observed during the initial cycles. At 5/5, charge/discharge became possible; however, the Coulombic efficiency remained low. Increasing the DMC fraction further improved the electrochemical response: the 4/6 ratio exhibited higher Coulombic efficiency, and the 3/7 ratio showed the most stable cycling behavior among the compositions tested (Fig. 1a).

Visual inspection revealed no apparent wetting at EC/DMC ratios of 6/4 and 5/5. Partial wetting was observed at 4/6, whereas complete wetting was achieved at 3/7 (Fig. 2).

Electrochemical performance correlated with the degree of separator wettability. At the 5/5 ratio, despite the absence of visible wetting immediately after electrolyte addition, charge/discharge was possible, suggesting delayed electrolyte penetration during the period between cell assembly and testing.

Overall, in the 1 M $LiPF_6$ system, improved Coulombic efficiency was obtained as the EC content decreased to 30 vol%, consistent with enhanced separator wettability, indicating that wettability is a key factor governing initial electrochemical performance.

Although this evaluation is qualitative, the observed trend was consistent across repeated measurements and correlated well with the electrochemical results shown in Fig. 1.

3.2. 1.8 M $LiPF_6$ EC/DMC or EC/EMC electrolyte system

To examine the influence of salt concentration, charge–discharge performance was evaluated using $LiPF_6$ electrolytes with concentrations up to 1.8 M and EC contents of ≤30 vol%.

Increasing the $LiPF_6$ concentration in EC/DMC = 3/7 from 1 M to 1.8 M resulted in lower Coulombic efficiency and poorer wettability of

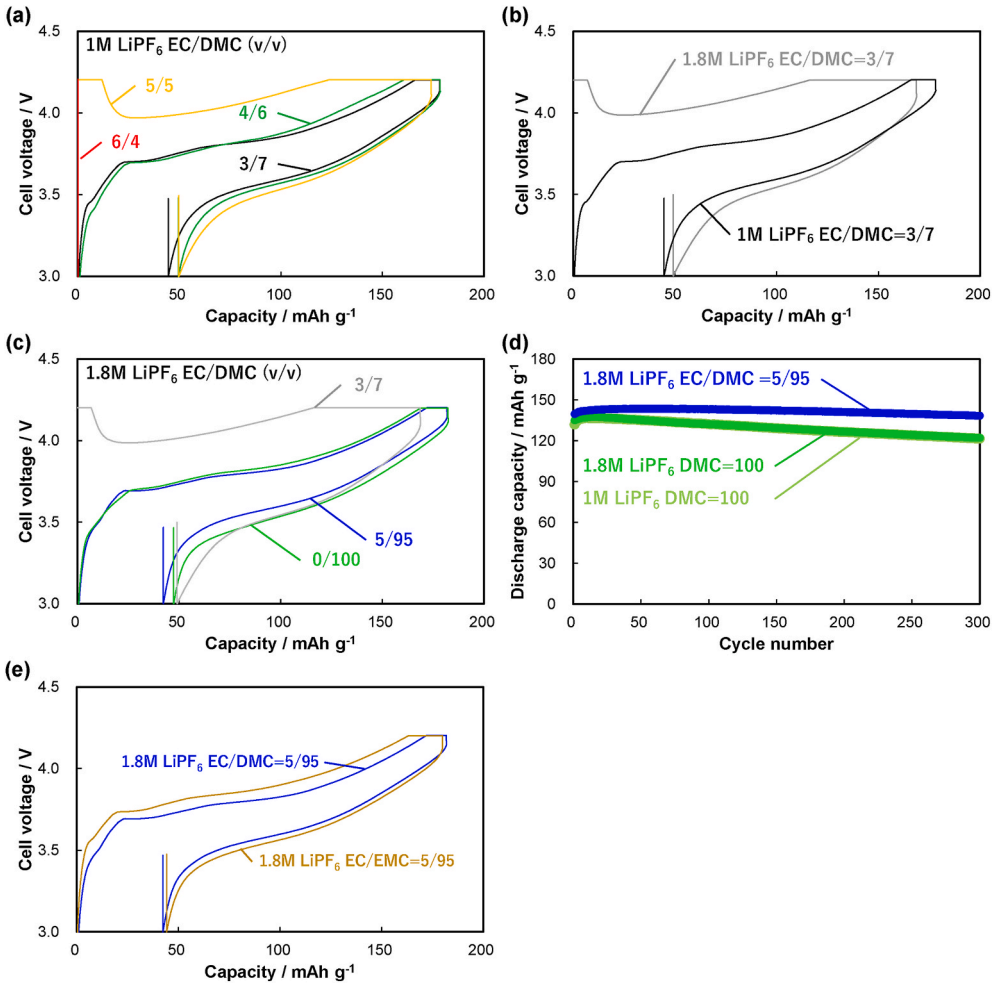

Fig. 1. First-cycle charge/discharge curves and cycling performance: (a) 1 M $LiPF_6$ in EC/DMC (by volume); (b) 1 M and 1.8 M $LiPF_6$ in EC/DMC = 3/7 (by volume); (c) 1.8 M $LiPF_6$ in EC/DMC (by volume); (d) 1 M and 1.8 M $LiPF_6$ in DMC (100 vol%) and 1.8 M $LiPF_6$ in EC/DMC = 5/95 (by volume); (e) 1.8 M $LiPF_6$ in EC/DMC = 5/95 and EC/EMC = 5/95 (by volume). All data were obtained at a 1C rate at 25 °C.

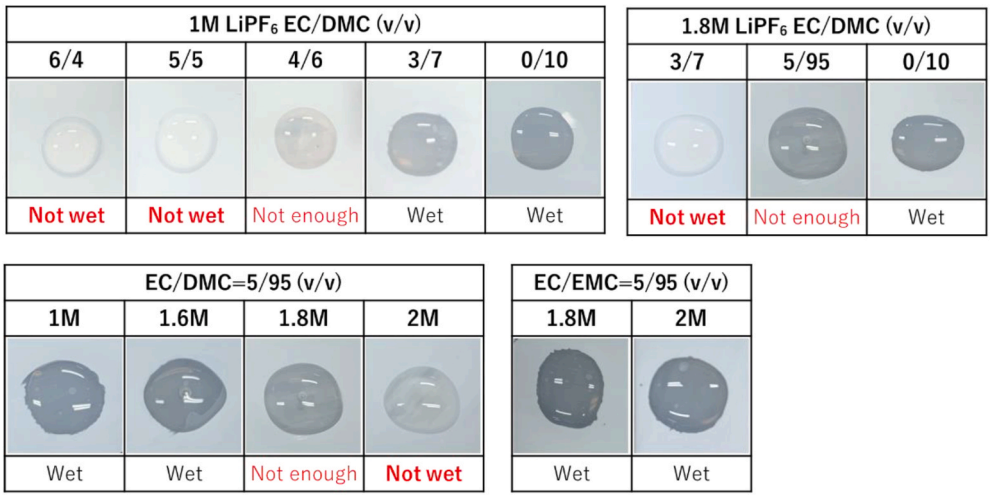

Fig. 2. Wettability of polyolefin separator.

the polyolefin separator (Fig. 1b and 2). In contrast, further reducing the EC fraction improved both Coulombic efficiency and separator wettability (Fig. 1c and 2).

Regardless of salt concentration, the EC-free electrolyte (EC/DMC = 0/10) exhibited inferior cycling stability. Introducing a small amount of EC (EC/DMC = 5/95) restored cycle performance (Fig. 1d), indicating that a limited EC content is still required for stable SEI formation. Although the viscosities of the two systems were comparable, the EC/DMC = 5/95 electrolyte showed higher ionic conductivity (Table 1).

However, in the EC/DMC = 5/95 system, separator wettability decreased as the $LiPF_6$ concentration exceeded 1.8 M (Fig. 2), suggesting that increased salt concentration hinders electrolyte penetration into the polyolefin separator. Replacing DMC with EMC at the same EC content (EC/EMC = 5/95) improved wettability, but slightly reduced Coulombic efficiency (Figs. 1 and 2), consistent with the higher viscosity and lower ionic conductivity of the EC/EMC system compared to EC/DMC (Table 1).

In addition, the electrolyte density tended to increase with increasing fractions of EC and DMC, whereas partial substitution of DMC with EMC at low EC content resulted in a slight reduction in the overall density.

These results highlight the trade-off between wettability, transport properties, and salt concentration in low-EC electrolyte design.

Wettability of polyolefin separator was discussed here based on electrochemical indicators, such as Coulombic efficiency and cycling behavior. Although EIS could provide additional insight, the consistent correlation between wettability, Coulombic efficiency, and cycling stability supports the present interpretation.

3.3. 1.8 M $LiPF_6$ EC/EMC/DMC = 5/10/85 electrolyte system

Fig. 3 shows the rate capability at 0 °C for cells with different electrolyte systems. The 1.8 M $LiPF_6$ in EC/EMC/DMC = 5/10/85 was compared with 1 M $LiPF_6$ in EC/EMC/DMC = 3/3/4, 3.7 M $LiPF_6$ in EC/EMC/DMC = 5/10/85, and highly concentrated LiFSI electrolytes in DMC (3.7 M, solvent/salt ratio = 2.2; 5.5 M, solvent/salt ratio = 1.1). In all cases, the charge and discharge C-rates were set to be identical.

To ensure a consistent basis for comparison, all measurements were conducted using identical cell configurations with a glass fiber separator, without polyolefin separators (PP/PE/PP), thereby minimizing differences in separator resistance. The highly concentrated LiFSI electrolytes were prepared using DMC as a representative low-viscosity linear carbonate solvent, which has been reported to favor high-rate performance compared to cyclic carbonates [19].

Under these conditions, the comparison primarily reflects differences in electrolyte properties. Among the electrolytes examined, 1.8 M $LiPF_6$ in EC/EMC/DMC = 5/10/85 exhibited the highest discharge capacity at high C-rates at 0 °C (Fig. 3), suggesting improved rate performance under low-temperature conditions relative to the other systems tested.

The effect of salt concentration was also evaluated by comparison with 3.7 M $LiPF_6$ in the same solvent system, while the LiFSI/DMC systems are included as reference examples of high-rate-oriented electrolyte design.

Although separator-related contributions are reduced in the present configuration, interfacial and electrode-related resistances may still influence the observed behavior. Therefore, the observed differences should be interpreted as reflecting overall cell performance under the

Table 1
Ionic conductivity, viscosity and density of the electrolytes at 25 °C.

Solvent (vol.%) / $LiPF_6$	Viscosity, mPa s			Conductivity, mS cm^{-1}			Density, g cm^{-3}		
	1.0M	1.8M	2.0M	1.0M	1.8M	2.0M	1.0M	1.8M	2.0M
DMC=100	1.7	4.1	5.3	7.0	9.9	9.6	1.171	1.252	1.270
EC/DMC=5/95	1.8	4.6	**5.8**	8.8	10.3	**9.7**	1.184	1.261	**1.280**
EC/EMC=5/95	2.3	6.0	7.8	5.9	6.3	5.8	1.131	1.210	1.228
EC/EMC/DMC=5/10/85	1.9	4.8	6.4	8.4	9.8	9.2	1.177	1.255	1.272
EC/EMC/DMC=3/3/4	3.0	-	-	10.7	-	-	1.229	-	-

Red: Not enough wetting; Red (**bold**): Not wet.

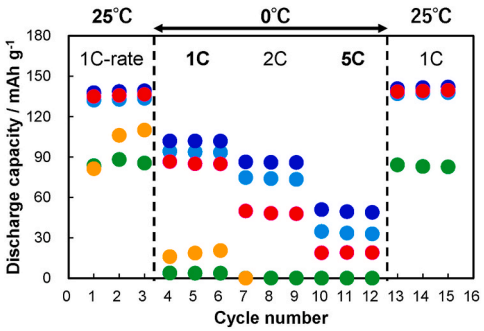

Electrolytes (vol.%)	5C/1C(%)	mPa s	mS cm^{-1}	g cm^{-3}
1M $LiPF_6$ EC/EMC/DMC=3/3/4	35	3.0	10.7	1.229
1.8M $LiPF_6$ EC/EMC/DMC=5/10/85	48	4.8	9.8	1.255
3.7M $LiPF_6$ EC/EMC/DMC=5/10/85	0	43	2.6	1.413
3.7M LiFSI DMC (solvent/salt ≈ 2.2)	22	41	3.4	1.420
5.5M LiFSI DMC (solvent/salt ≈ 1.1)	-	301	0.91	1.567

All without separators

Fig. 3. C-rate performance (1C, 2C, and 5C) at 0 °C, and viscosity, ionic conductivity and density at 25 °C.

present conditions.

This behavior can be attributed to the higher lithium-ion concentration of the 1.8 M electrolyte relative to the 1 M system, while maintaining comparable ionic conductivity and viscosity. In contrast, 3.7 M LiFSI in DMC contains a higher lithium-ion concentration but exhibits lower ionic conductivity and higher viscosity at 25 °C, which likely limits ion transport under high-rate conditions. The 5.5 M LiFSI system shows a further decrease in ionic conductivity and increase in viscosity, consistent with its inferior rate performance.

3.4. *Melting point and flash point of 1.8 M $LiPF_6$ EC/EMC/DMC = 5/10/85*

Because EC and DMC account for 90 vol% of the EC/EMC/DMC = 5/10/85 electrolyte and have melting points of 36 °C and 3 °C, respectively, the low-temperature phase behavior was evaluated at −20 °C (Fig. 4).

For the 1 M system, solidification occurred at −20 °C when the combined EC and DMC content exceeded 70 vol%, indicating that the high fraction of relatively high-melting components dominates the phase behavior. In contrast, the 1.8 M $LiPF_6$ EC/EMC/DMC = 5/10/85 electrolyte remained fully liquid under the same conditions. These results suggest that the wettability-optimized composition is also beneficial for suppressing freezing at −20 °C.

In contrast, the flash point of the EC/EMC/DMC = 5/10/85 electrolyte at 1 M $LiPF_6$ was 20 °C, reflecting the high DMC content (flash point: 17–18 °C). When the salt concentration was increased to 1.8 M, the flash point increased to 24 °C. This increase is consistent with reduced volatility at higher salt concentration.

Overall, increasing the salt concentration not only improves low-temperature fluidity but also enhances safety by elevating the flash point, suggesting an additional advantage of high-concentration electrolyte design.

3.5. *The cycling performance of 1.8 M Li salt EC/EMC/DMC = 5/10/85*

First, the cycling performance of 1 M $LiPF_6$ and 1 M LiFSI in EC/EMC/DMC = 5/10/85 was evaluated at 25 °C and compared with a commonly used conventional electrolyte, 1 M $LiPF_6$ in EC/EMC/DMC = 3/3/4, to provide a relevant reference for performance evaluation. As shown in Fig. 5a, both electrolyte systems exhibited stable cycling behavior over 300 cycles under these conditions.

Next, the salt concentration was increased to 1.8 M for both $LiPF_6$ and LiFSI in EC/EMC/DMC = 5/10/85. These electrolytes also maintained stable cycling performance over 300 cycles. In contrast, 1.8 M LiFSI in EC/DMC = 3/7 (30 vol% EC) showed relatively lower cycling stability, despite the identical salt concentration (Fig. 5b). This result suggests that solvent composition plays an important role in determining cycling behavior. The difference may be associated with variations in Li^+ solvation structure and related interfacial processes. These findings suggest that wettability-optimized solvent compositions contribute to stable electrode/electrolyte behavior across different salt systems.

At 60 °C and 4.2 V, NCM523/graphite full cells with the 1 M LiFSI electrolyte retained 80% of their initial capacity after 300 cycles, whereas the 1.8 M LiFSI electrolyte showed slightly improved cycling performance of 84%. This trend suggests that moderate salt concentration may be beneficial under elevated-temperature conditions. The improved performance of LiFSI-based electrolytes at high temperature is generally attributed to their relatively high thermal stability and ionic

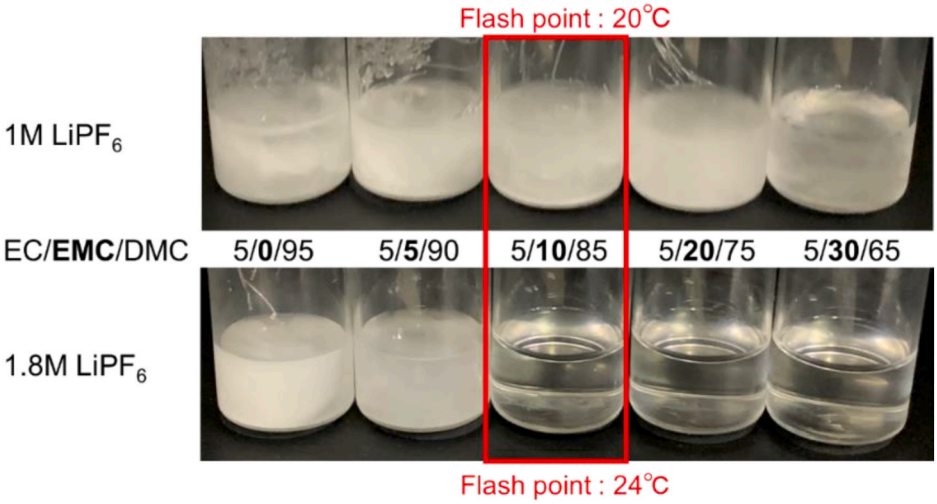

Fig. 4. Freezing test at −20 °C (1 M or 1.8 M $LiPF_6$ in EC/EMC/DMC, by volume).

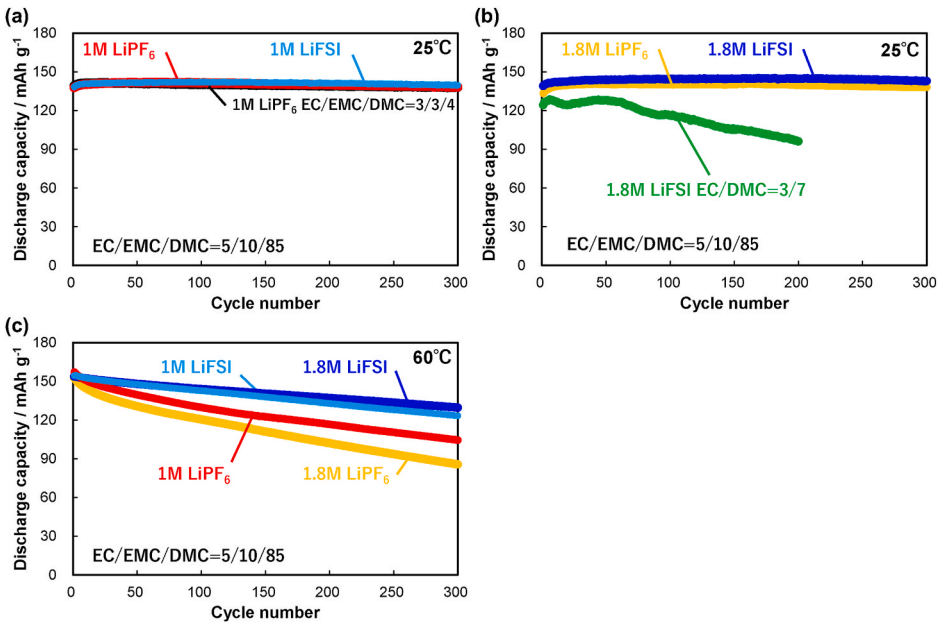

Fig. 5. 1C cycling performance of $LiPF_6$ and LiFSI at (a, b) at 25 °C and (c) at 60 °C for 300 cycles.

conductivity, as well as the formation of LiF-rich interfacial layers reported in previous studies [24–26].

In contrast, $LiPF_6$-based electrolytes showed lower capacity retention at elevated temperature. The retention after 300 cycles was 67% for the 1 M system and 56% for the 1.8 M system. This behavior may be related to the thermal instability of $LiPF_6$, which can generate reactive species such as PF_5 and HF at elevated temperatures, potentially accelerating interfacial degradation, particularly at higher salt concentrations.

Elevated-temperature cycling is commonly used as an accelerated aging method; therefore, the present results provide an indication of longer-term stability, although the quantitative lifetime depends on the cell system.

As noted in the Introduction, LiFSI-based electrolytes at conventional or moderately concentrated levels (e.g., 1–2 M), rather than in highly concentrated systems, are known to induce corrosion of the Al cathode current collector. This issue arises from the insufficient formation of a protective passivation layer on Al in the presence of FSI^--derived species, and remains a critical limitation for practical applications.

Therefore, while LiFSI provides clear advantages in terms of high-temperature cycling performance, its practical implementation requires careful electrolyte design to mitigate Al corrosion, particularly in moderately concentrated electrolyte systems.

In this context, the present results demonstrate that LiFSI-based electrolytes at moderate concentrations (1–2 M) can also exhibit stable cycling behavior under appropriate solvent compositions. Based on this observation, a systematic investigation of the relationship between EC content and salt concentration was conducted.

3.6. Al corrosion behavior of LiFSI electrolytes

In this section, a simplified model electrolyte system was employed to systematically investigate the effects of EC content and salt concentration. EMC was intentionally excluded to reduce compositional complexity. As a linear carbonate similar to DMC, the addition of EMC is expected to mainly influence bulk properties such as viscosity and wettability through dilution effects, while its impact on Al corrosion behavior is considered secondary. Therefore, the EC/DMC-based model system is used here as a simplified framework to examine the relationships between solvent composition and Al corrosion.

To clarify the relationship between solvent composition and Al corrosion in LiFSI-based electrolytes, EC fractions and salt concentrations were systematically varied. Electrolytes of 1 M LiFSI in EC/DMC = 1/9, 2/8, and 3/7, and EC/GBL = 3/7 (Fig. 6a), as well as 1.8 M and 3.7 M LiFSI in EC/DMC = 3/7 (Fig. 6b), were examined. The electrolytes 1 M LiFSI EC/GBL = 3/7, 1.8 M LiFSI EC/DMC = 3/7, and 3.7 M LiFSI EC/DMC = 3/7 did not wet the polyolefin separator; therefore, glass fiber separators were used in these experiments to ensure sufficient electrolyte uptake. To minimize possible corrosion of the SUS316L coin cell cases [23], an Al foil was inserted between the cathode and the case (see Section 2.4).

At 25 °C, cycling stability decreased with increasing EC content. The EC/GBL = 3/7 system exhibited the poorest performance (Fig. 6a), suggesting that high fractions of cyclic, high-dielectric solvents may accelerate degradation. Increasing the salt concentration from 1 M to 1.8 M in EC/DMC = 3/7 slightly improved stability; however, the performance remained lower than that of the highly concentrated 3.7 M electrolyte (Fig. 6b), suggesting that concentration alone may be insufficient to fully suppress degradation.

LSV was conducted to evaluate the initial Al dissolution behavior. In Fig. 6d, higher dissolution currents were observed for electrolytes exhibiting poorer cycling performance; however, no clear trend was identified in Fig. 6c. This discrepancy indicates that LSV reflects only initial behavior, whereas cycling degradation depends on cumulative corrosion.

To directly evaluate long-term corrosion, the amount of Al deposited on the graphite anode after 200 cycles was quantified by ICP analysis. In contrast to LSV, the ICP results suggest a positive correlation between Al deposition and the presence of high-dielectric cyclic solvents such as EC and GBL (Fig. 6e). While the dataset is limited, this trend is consistent with both LSV results and cycling performance, supporting a phenomenological interpretation.

Although the moderately concentrated 1.8 M electrolyte did not suppress Al deposition to the same extent as the super-highly concentrated system (Fig. 6f), limiting high-dielectric cyclic solvents to ≤5 vol % markedly reduced cumulative Al deposition while maintaining stable cycling behavior.

These results suggest that cycling deterioration in LiFSI-based electrolytes is closely associated with cumulative Al corrosion and that solvent composition plays an important role in controlling long-term dissolution behavior. In particular, minimizing high-dielectric cyclic

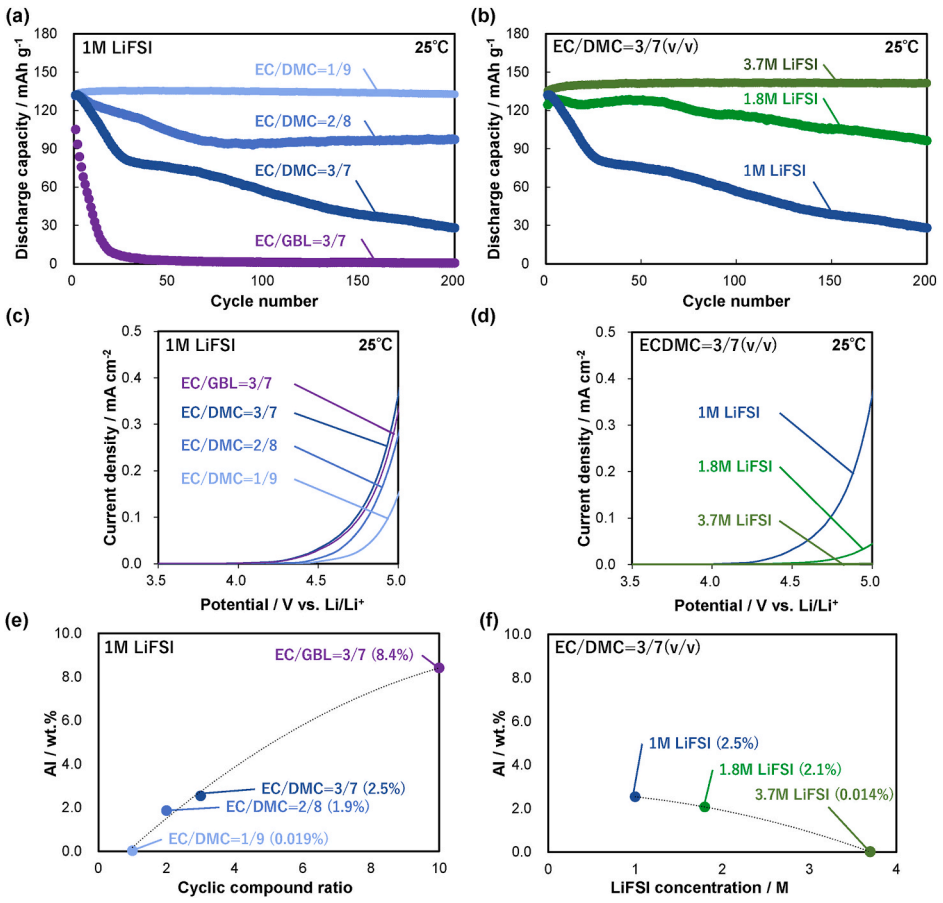

Fig. 6. (a, b) 1C cycling performance at 25 °C. (c, d) LSV using an Al electrode at 25 °C. (e, f) Amount of Al deposited per gram of graphite after 200 cycles, as determined by ICP-AES. (a, c, e) 1 M LiFSI; (b, d, f) EC/DMC = 3/7.

solvents appears to be an effective strategy to suppress Al corrosion without resorting to super-high salt concentrations.

The present study does not include surface characterization such as XPS or SEM; therefore, the interpretation is limited to phenomenological correlations.

3.7. Factors inhibiting Al corrosion

Previous studies have suggested that oxidation of cyclic carbonate solvents such as EC can generate protonic or other reactive species that chemically dissolve Al at high potentials [27]. Mori et al. demonstrated that decreasing EC content, while increasing the fraction of low-dielectric solvents such as tetrahydrofuran and 1,2-dimethoxyethane, suppresses Al corrosion in lithium bis(trifluoromethanesulfonyl)imide (LiTFSI)-based systems [4]. Winter et al. showed that EC-free EMC-based electrolytes containing 1 M $LiPF_6$ improve interfacial stability compared with EC-containing formulations [15]. Although these studies employed different lithium salts (LiTFSI or $LiPF_6$), they consistently indicate that reducing the fraction of high-dielectric cyclic solvents contributes to enhanced interfacial stability and mitigated metal dissolution.

In LiFSI-based electrolytes, suppression of Al corrosion has typically relied on super-high salt concentrations [18] or on the use of additive salts such as lithium difluoro(oxalato)borate (LiDFOB), lithium tetrafluoroborate ($LiBF_4$), or lithium difluorophosphate ($LiPO_2F_2$) [28,29], which are generally considered to promote the formation of protective surface layers on Al.

In contrast, the present results suggest that Al corrosion can be mitigated without additives and without resorting to super-high salt concentrations, provided that the fraction of high-dielectric cyclic solvents is minimized. Specifically, restricting EC to ≤5 vol% in a DMC-rich electrolyte markedly reduces cumulative Al deposition even in a moderately concentrated (1.8 M) system.

These findings indicate that solvent composition plays an important role in determining Al corrosion behavior in LiFSI electrolytes, alongside the influence of salt concentration in the moderate concentration regime. Although the detailed dissolution mechanism remains under discussion, the present results are consistent with a practical design principle: maintaining only a minimal amount of EC required for stable SEI formation, while limiting the contribution of cyclic solvents to Al dissolution.

This approach may provide an alternative strategy to conventional high-concentration or additive-based solutions for mitigating Al corrosion.

It should be noted that the present discussion is based on phenomenological correlations between electrolyte composition, cumulative Al dissolution (ICP), and cycling performance, and does not include direct surface characterization of the passivated Al (e.g., SEM or XPS). Therefore, this study provides practical design guidance, although detailed mechanisms remain beyond the scope of this work.

3.8. Conductivity and viscosity at LiFSI EC/EMC/DMC = 5/10/85 system

As shown in Fig. 7a, the EC/EMC/DMC = 5/10/85 electrolyte exhibited lower viscosity than the conventional EC/DMC = 1/2 system. This reduction is attributed to the decreased fraction of high-viscosity EC and the increased proportion of low-viscosity linear carbonates such as DMC and EMC.

Correspondingly, the maximum ionic conductivity shifted from

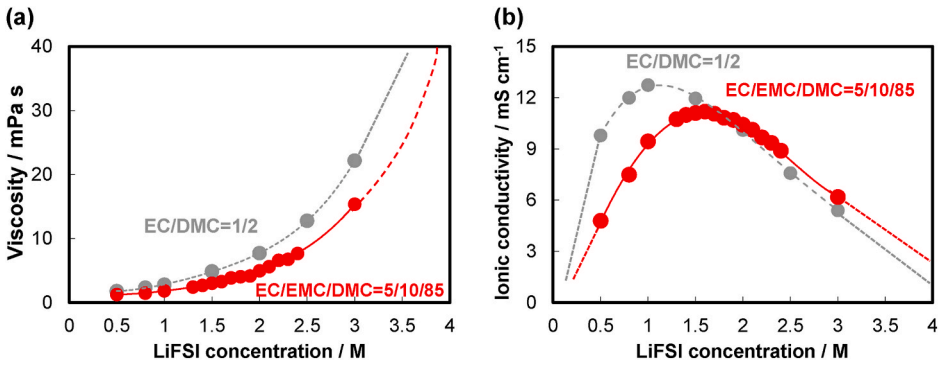

Fig. 7. Viscosity and ionic conductivity of the LiFSI-based electrolytes at 25 °C.

approximately 1.0 M in the EC/DMC system to around 1.8 M in the EC/EMC/DMC system (Fig. 7b). This shift suggests that the optimized solvent composition enables efficient ion transport even at moderately elevated salt concentrations.

The shift in the conductivity maximum can be rationalized in terms of changes in Li^+ solvation and ion-pairing behavior. In EC-rich systems, strong Li^+ solvation tends to stabilize dissociated ionic species at low concentrations, whereas increasing salt concentration promotes the formation of ion-associated species, which can reduce ionic mobility and conductivity above ~1.0 M.

As a result, the 1.8 M LiFSI EC/EMC/DMC = 5/10/85 electrolyte achieves a favorable balance between lithium-ion concentration, ionic conductivity, and viscosity, which is consistent with the improved rate capability and cycling performance described above.

4. Conclusion

In this study, practical electrolyte design was investigated by focusing on two key parameters: (i) EC content and (ii) Li salt concentration, through systematic evaluation.

Reducing the EC content to 5 vol% improved separator wettability and lowered viscosity while maintaining sufficient ionic conductivity. Under the present conditions, limiting the fraction of cyclic carbonate solvents was also associated with reduced Al dissolution in LiFSI-based electrolytes.

With respect to salt concentration, the 1.8 M LiFSI in EC/EMC/DMC = 5/10/85 electrolyte (solvent/salt ratio of 4.5) exhibited a well-balanced set of properties, including sufficient wettability, no freezing at −20 °C, an increased flash point relative to the 1 M system, and favorable rate capability. In NCM523/graphite full cells operated at 4.2 V and 60 °C, this electrolyte retained 84% of its initial capacity after 300 cycles, compared with 56% for the corresponding $LiPF_6$-based electrolyte.

Although LiFSI at moderate concentrations (1–2 M) is generally associated with Al corrosion, restricting cyclic carbonate solvents to ≤5 vol% was found to mitigate this behavior under the present conditions. Furthermore, increasing salt concentration appears to compensate for reduced EC content by maintaining ionic availability while preserving favorable transport properties.

Overall, this study identifies a practical compositional window for LiFSI-based electrolytes that balances transport properties and corrosion behavior without relying on superconcentrated formulations. While further mechanistic investigation is required, the present results provide a useful guideline for electrolyte design.

CRediT authorship contribution statement

Yuji Ide: Conceptualization, Data curation, Formal analysis, Investigation, Methodology, Validation, Visualization. **Yanko Marinov Todorov:** Conceptualization, Data curation, Formal analysis, Investigation, Methodology, Validation, Writing – review & editing. **Masaki Deguchi:** Conceptualization, Investigation, Methodology, Resources, Validation, Writing – review & editing. **Koji Abe:** Conceptualization, Funding acquisition, Investigation, Methodology, Project administration, Resources, Supervision, Writing – original draft, Writing – review & editing.

Declaration of competing interest

The authors declare that they have no known competing financial interests or personal relationships that could have appeared to influence the work reported in this paper.

Data availability

Data will be made available on request.

References

[1] E. Peled, J. Electrochem. Soc. 126 (1979) 2047, https://doi.org/10.1149/1.2128859.
[2] R. Fong, U. von Sacken, J.R. Dahn, J. Electrochem. Soc. 137 (1990) 2009, https://doi.org/10.1149/1.2086855.
[3] K. Kanamura, T. Okagawa, Z. Takehara, J. Power Sources 57 (1995) 119, https://doi.org/10.1016/0378-7753(95)02265-1.
[4] X. Wang, E. Yasukawa, S. Mori, Electrochim. Acta 45 (2000) 2677, https://doi.org/10.1016/S0013-4686(99)00429-6.
[5] E. Rao, B. McVerry, A. Borenstein, M. Anderson, R.S. Jordan, R.B. Kaner, ACS Appl. Energy Mater. 1 (2018) 3292, https://doi.org/10.1021/acsaem.8b00502.
[6] M. Deguchi, D. Tazoe, Y.M. Todorov, K. Abe, J. Electrochem. Soc. 171 (2024) 040536, https://doi.org/10.1149/1945-7111/ad39cb.
[7] Gaurav Sharma, Yi Jin, Y.S. Lin, J. Electrochem. Soc. 164 (6) (2017) A1184, https://doi.org/10.1149/2.1091706jes.
[8] L. Zhu, G. Ding, Q. Han, X. Yang, L. Xie, X. Cao, J. Electrochem. Soc. 168 (2021) 100524, https://doi.org/10.1149/1945-7111/ac2dca.
[9] R. Petibon, J. Xia, L. Ma, M.K.G. Bauer, K.J. Nelson, J.R. Dahn, J. Electrochem. Soc. 163 (13) (2016) A2571, https://doi.org/10.1149/2.0321613jes.
[10] L. Ma, S.L. Glazier, R. Petibon, J. Xia, J.M. Peters, Q. Liu, J. Allen, R.N.C. Doig, J. R. Dahn, J. Electrochem. Soc. 164 (2017) A5008, https://doi.org/10.1149/2.0191701jes.
[11] W. Li, A. Dolocan, J. Li, Q. Xie, A. Manthiram, Adv. Energy Mater. 9 (2019) 1901152, https://doi.org/10.1002/aenm.201901152.
[12] R. Pan, Z. Cui, M. Yi, Q. Xie, A. Manthiram, Adv. Energy Mater. 12 (2022) 2103806, https://doi.org/10.1002/aenm.202103806.
[13] J.S. Terreblanche, T. Luo, L.F.J. Piper, W.M. Dose, Adv. Energy Mater. 15 (2025) 2404427, https://doi.org/10.1002/aenm.202404427.
[14] J. Xia, R. Petibon, D. Xiong, L. Ma, J.R. Dahn, J. Power Sources 328 (2016) 124, https://doi.org/10.1016/j.jpowsour.2016.08.015.
[15] E.R. Logan, E.M. Tonita, K.L. Gering, L. Ma, M.K.G. Bauer, J. Li, L.Y. Beaulieu, J. R. Dahn, J. Electrochem. Soc. 165 (2018) A705, https://doi.org/10.1149/2.0981803jes.
[16] S. Klein, S. Wickeren, S. Röser, P. Bärmann, K. Borzutzki, B. Heidrich, M. Börner, M. Winter, T. Placke, J. Kasnatscheew, Adv. Energy Mater. 11 (2021) 2003738, https://doi.org/10.1002/aenm.202003738.
[17] S. Uchida, M. Ishikawa, J. Power Sources 359 (2017) 480, https://doi.org/10.1016/j.jpowsour.2017.05.090.
[18] Y. Yamada, Bull. Chem. Soc. Jpn. 93 (2020) 109, https://doi.org/10.1246/bcsj.20190314.
[19] J. Wang, Y. Yamada, K. Sodeyama, C.H. Chiang, Y. Tateyama, A. Yamada, Nat. Commun. 7 (2016) 12032, https://doi.org/10.1038/ncomms12032.

[20] Y. Yamada, A. Yamada, J. Electrochem. Soc. 162 (2015) A2406, https://doi.org/10.1149/2.0041514jes.
[21] S. Wang, Z. Xue, F. Chu, Z. Guan, J. Lei, F. Wu, J. Energy Chem. 79 (2023) 201, https://doi.org/10.1016/j.jechem.2022.12.060.
[22] K. Miura, M. Deguchi, Y.M. Todorov, K. Abe, Electrochim. Acta 539 (2025) 147054, https://doi.org/10.1016/j.electacta.2025.147054.
[23] X. Wu, Z. Du, Electrochem. Commun. 129 (2021) 107088, https://doi.org/10.1016/j.elecom.2021.107088.
[24] H.B. Han, S.S. Zhou, D.J. Zhang, S.W. Feng, L.F. Li, K. Liu, W.F. Feng, J. Nie, H. Li, X.J. Huang, M. Armand, Z. Bin Zhou, J. Power Sources 196 (2011) 3623, https://doi.org/10.1016/j.jpowsour.2010.12.040.
[25] Z. Du, D.L. Wood, I. Belharouak, Electrochem. Commun. 103 (2019) 109, https://doi.org/10.1016/j.elecom.2019.04.013.
[26] S.J. Kang, K. Park, S.H. Park, H. Lee, Electrochim. Acta 259 (2018) 949, https://doi.org/10.1016/j.electacta.2017.11.018.
[27] T. Ma, G.-L. Xu, Y. Li, L. Wang, X. He, J. Zheng, J. Liu, M.H. Engelhard, P. Zapol, L. A. Curtiss, J. Jorne, K. Amine, Z. Chen, J. Phys. Chem. Lett. 8 (2017) 1072, https://doi.org/10.1021/acs.jpclett.6b02933.
[28] K. Park, S. Yu, C. Lee, H. Lee, J. Power Sources 296 (2015) 197, https://doi.org/10.1016/j.jpowsour.2015.07.052.
[29] M. Deguchi, Y.M. Todorov, K. Abe, Electrochim. Acta 469 (2023) 143267, https://doi.org/10.1016/j.electacta.2023.143267.